

Monte Carlo Implementation for Simulation of Ostwald Ripening Via Long Range Diffusion in Two-Phase Solids

Rifa J. El-Khozondar¹, Hala J. El-Khozondar²

¹Physics Department, Applied Science College/ Al-Aqsa University, Palestine

²Electrical Engineering Department, Engineering College/ Islamic University of Gaza, Palestine

Abstract: Numerical simulations based on the Monte Carlo Potts model are used to study coupling of grain growth and Ostwald ripening in two-phase polycrystalline materials. The ratio of the grain boundary energy to the interphase boundary energy is used as an input parameter. It is shown that the grain growth in two-phase polycrystalline materials is controlled by long-range diffusion and the change of the mean grain size with time obeys the growth law, $\langle R \rangle^n = \langle R \rangle_0^n + kt$ where n is the grain growth exponent. The value of n is calculated for a broad series of volume fractions. It is found that the inverse grain growth exponent, $1/n$, in agreement with the theoretical value, $1/n=1/3$, noticed during computer simulations for volume fractions between 40% and 90%. However, the value of $1/n$ is smaller than $1/3$ for volume fractions between 10% and 30%. Furthermore, the temporal development of the number of grains has been analyzed for the entire range of volume fractions. It is also seen that the quasi-stationary state is advanced at varied aging times depending on the volume fractions. Furthermore, it is shown that the simulated size distribution are symmetric and peaked at $x=1$ for volume fractions differ between 50% and 90%; however, the simulated size distribution become asymmetric and skew to smaller grains for lower volume fractions change between 10% and 40%.

Keywords: Monte Carlo, Ostwald Ripening, Polycrystalline Materials, Grain Growth, Volume Diffusion

I. Introduction

The grain size controls the thermal, electrical and mechanical properties of polycrystalline materials. This emphasizes that the grain size plays an important role of improving materials properties during processing. Therefore, understanding microstructural evolution and Ostwald ripening in two-phase materials is a key topic for applications of engineering materials. It is well known that the polycrystalline microstructures do not comprise grains of one size, but can relatively be defined mean grain size and grain size distribution. The average grain size varies with time according to the power-law function

$$\langle R \rangle = \left(\langle R \rangle_0^n + kt \right)^{1/n} \quad (1)$$

where k is the grain growth constant. The theoretical value of n is 2 for pure metals [1-3]. However, for Ostwald ripening, $n=3$ for long-range diffusion [4,5] and $n=4$ for grain boundary diffusion [6]. Simultaneously, the grain structure evolves to quasi-stationary state in which the grain size distribution are stationary and indistinguishable from each other. The total number of grains drops as grain growth continues and can be described by the following equation

$$N = \frac{A}{\langle A \rangle} = \frac{A}{4\pi \langle R^2 \rangle} = \frac{A}{4\pi \langle x^2 \rangle \langle R \rangle^2} \quad (2)$$

where the scaled grain radius, $x=R/\langle R \rangle$. Replacing $\langle R \rangle$ from (1) into (2) gives the fitting relationship

$$N(t) = (kt + C)^\alpha \quad (3)$$

where the exponent α has the value of $-2/3$ when microstructural evolution is controlled by Ostwald ripening via long-range diffusion. The grain size distribution as a function of the scaled grain radius have been derived by several authors [6-8].

In two-phase materials such as ceramics and metallic alloys [9, 10], grain growth and Ostwald ripening may occur simultaneously. These materials have important applications in electronic industries. There have been experimental attempts [11-17] and numerical simulations [18-21] to study the coupling between grain growth and Ostwald ripening.

In this work, the Monte Carlo Potts model adjusted by Solomatov et al. [20] to study grain growth in two-phase polycrystalline materials is developed to study Ostwald ripening via long-range diffusion in two-phase polycrystalline materials. The model is comparable to one established by El-Khozondar and El-Khozondar [22] for Ostwald ripening of solid grains in a liquid matrix. However, in the present work the second phase is solid which has grain boundaries. The Monte Carlo Potts model has shown to be successful to simulate grain growth in polycrystalline materials for one, two and three phases [23-37]. The modified Monte Carlo model in this work allows us to display microstructural evolution of polycrystalline materials and gives us information about the average grain size and the grain size distribution. Therefore, the grain growth exponent can be calculated from the simulation results. Next section will focus on the simulation model. Section III is dedicated to the Simulation of Ostwald ripening in two-phase systems. Conclusion is presented in section VI.

II. The Simulation Model

The The Monte Carlo Potts is adapted to simulate Ostwald ripening in two-phase polycrystalline materials. The simulation is initiated using a quadratic lattice with eight nearest neighbors. Every lattice point is named one Monte Carlo Unit. In the current simulation, the number of Monte Carlo Units of the simulated microstructure is taken to be 400×400. The unit of time is given in Monte Carlo steps (MCS) which signifies N orientation attempts where N is equivalent to the number of Monte Carlo Units. This implies that N=16,000 in our simulations.

The original microstructure of two-phase system is treated as a two-dimensional square array of Monte Carlo Units. Each Monte Carlo Unit is given a random number between 1 and Q where Q is the number of orientations. The value Q=100 is used in our simulations. The Monte Carlo Units of phase A are given positive numbers. The Monte Carlo Units of phase B are given negative numbers. A grain comprises a group of Monte Carlo Units with similar orientations. A grain boundary is then an edge, which separates grains with different orientations.

There are three kinds of boundaries. The grain boundaries between grains in phase A have energy Eaa. The grain boundaries between grains in phase B have energy Ebb. The interphase boundaries between grains in phase A and grains in phase B have energy Eab. The values of the interfacial energies are selected such that the values of the grain boundary energies (Eaa and Ebb) are greater than the value of Eab. Ostwald ripening is simulated using Eaa=2.5, Ebb=2.5 and Eab=1.

The change of the two-phase microstructure is motivated by the decrease in the entire energy of grain and interphase boundary. It includes two processes: grain boundary migration and Ostwald ripening by long-range diffusion. Grain boundary migration happens because of orientation flip in one phase as follows. One Monte Carlo unit is randomly selected and is flipped to a different randomly selected orientation. Then, the difference in energy ΔE is calculated. The new orientation is selected using the next rule: If $\Delta E \leq 0$, the flip is accepted; however, if $\Delta E > 0$, the flip is rejected. The second process is Ostwald ripening by long-range diffusion that moves material from one grain to another grain of the same phase through the grains of the other phase.

This is numerically done by using orientation exchange between the phases as follows. One Monte Carlo unit and its neighbor are selected in a probabilistic way. If they belong to different phases, they are permitted to exchange their orientations. The energy difference is then calculated. The new orientation of the two Monte Carlo Units is chosen by the following rule. If $\Delta E \leq 0$, the exchange is accepted. Conversely, if $\Delta E > 0$, the exchange is accepted with the following exchange probability function.

$$P = \exp\left(-\frac{\Delta E}{kT}\right) \quad (3)$$

where k is the Boltzman constant and T is the temperature. The temperature has the value of T=1.3. After each attempt, the time is incremented by 1/N MCS.

III. Simulation of Ostwald Ripening in Two-Phase Systems

Fig. 1 exhibits the temporal microstructural evolution in two-phase system for different volume fractions. The volume fraction of the B phase (white grains) varies between 10% and 50% as well as the volume fraction of the A phase (grey grains) varies between 50% to 90%. As can be seen from Fig. 1 that there is an indication of Ostwald ripening where the number of grains declines and the mean grain size grows with time. Moreover, the microstructure evolves because of moving atoms from small grains to large grains via volume diffusion. Consequently, small grains ultimately contract and large grains grow in size.

Fig. 2 displays the time dependence of the number of grains for the whole range of volume fractions. It can be shown from Fig. 2 that the number of grains drops (solid line) following the quasi-stationary state (4) with the value of exponent from numeric fit (dashed line) equivalents to -2/3. Additionally, it can be observed from Fig.

2 that the quasi-stationary state is progressed at varied aging times depending on the volume fraction of the case. The quasi-stationary state is attained near the end of simulation time, $t > 50000$ MCS when volume fractions have values of 10%, 20%, and 30%. Whereas the quasi-stationary state is advanced at $t > 7000$ MCS for volume fractions with values equivalent to 40%, 50%, and 60%. When volume fractions are equal to 70%, 80%, and 90%, the quasi-stationary state is arrived at $t > 1000$ MCS. It can be concluded that as the volume fraction increases, the quasi-stationary state is reached at earlier times and vice versa.

Fig. 3 shows the change of average grain size with time for the entire series of volume fractions. The average grain size and the standard deviation are calculated after running each case ten times. The standard deviation is not indicted because it is found to be very small. It is noticed from Fig. 3 that the system goes through a transitional regime and eventually approach the quasi-stationary state at different times depending on the case of volume fraction. The value of the growth exponent is calculated by taking the slope of the curves shown in Fig. 3. The slope is calculated in a time gap which moving across the time axis because the growth exponent is very sensitive to time variation. The logarithmic size of the time gap is equivalent to 5. The slope is plotted against time in Fig. 4. It can be seen from Fig. 4 that for volume fractions vary between 40% and 90%, the slope in the quasi-stationary state is close to the theoretical value $1/3$ projected for Ostwald ripening via long-range diffusion. However, the slope is lower than the theoretical value $1/3$ for volume fractions differ between 10% and 30%.

Fig. 5 and Fig. 6 depict the temporal development of the scaled grain size distribution at five different time steps for a range of volume fractions of phase B varies between 10%-50% for phase B and for a range of volume fractions of phase A varies between 50%-90%. It is shown from these figures that the size distribution are identical for volume fractions vary between 50% and 90% and coincide with the normal distribution function. Additionally, the simulated size distributions are peaked at $x=1$ and symmetric. While the simulated size distribution within are asymmetric and skew to smaller grains for lower volume fractions differ between 10% and 40%.

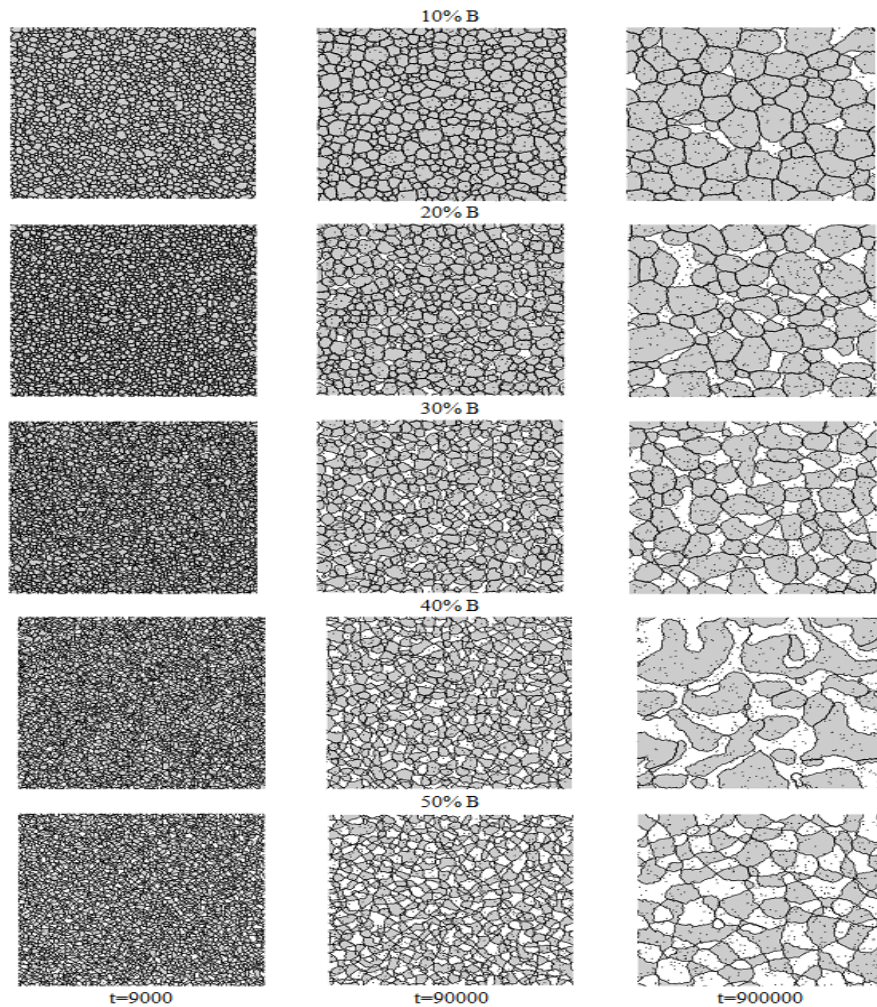


Fig. 1 Simulated microstructure of a system comprising two-phase polycrystalline material, phase A (grey) and phase B (white), for different volume fractions of the B phase.

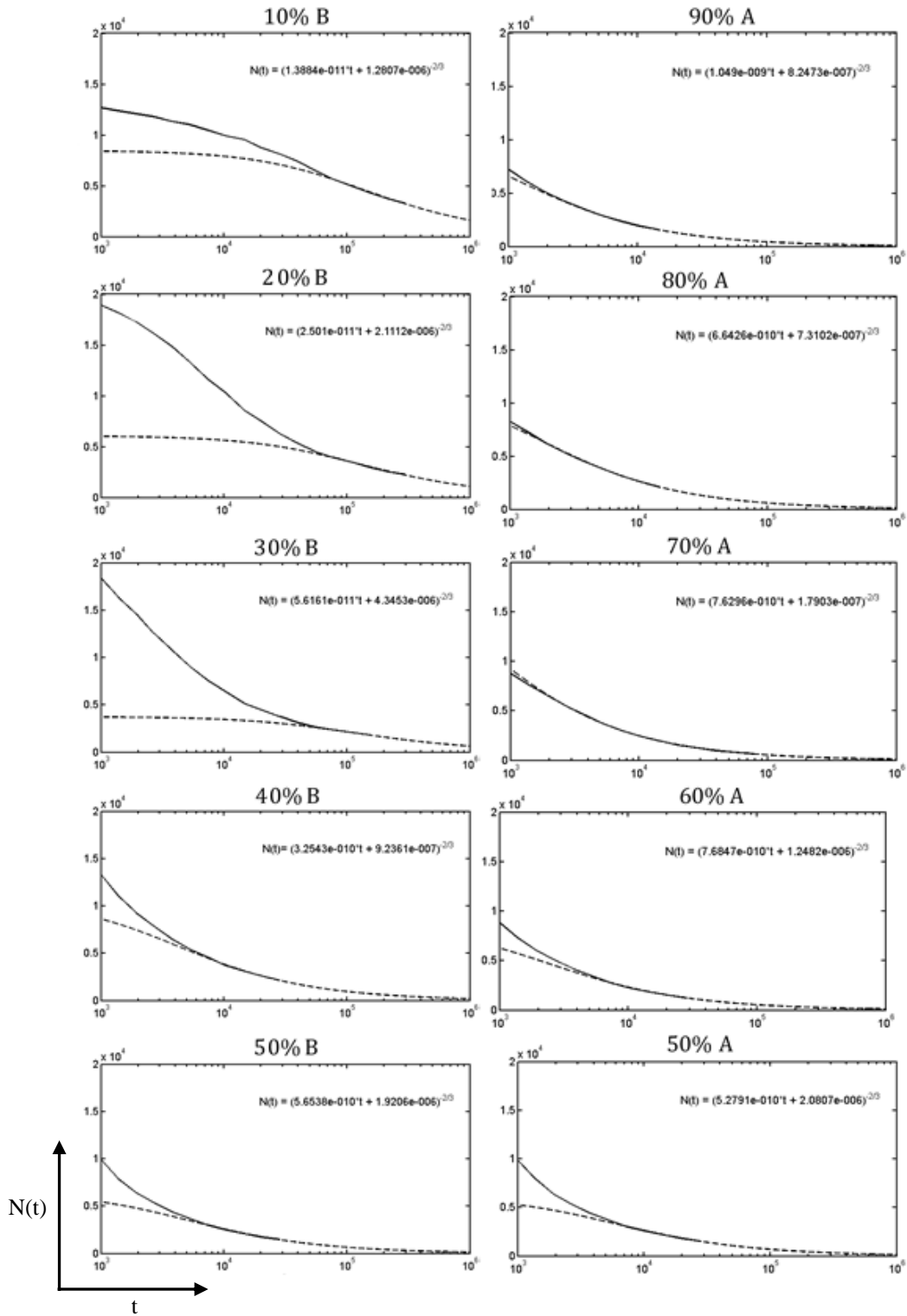


Fig. 2. Variation of the number of grains (N) with time for a varied volume fraction of the B phase (solid line) with fit to (3) (dashed line).

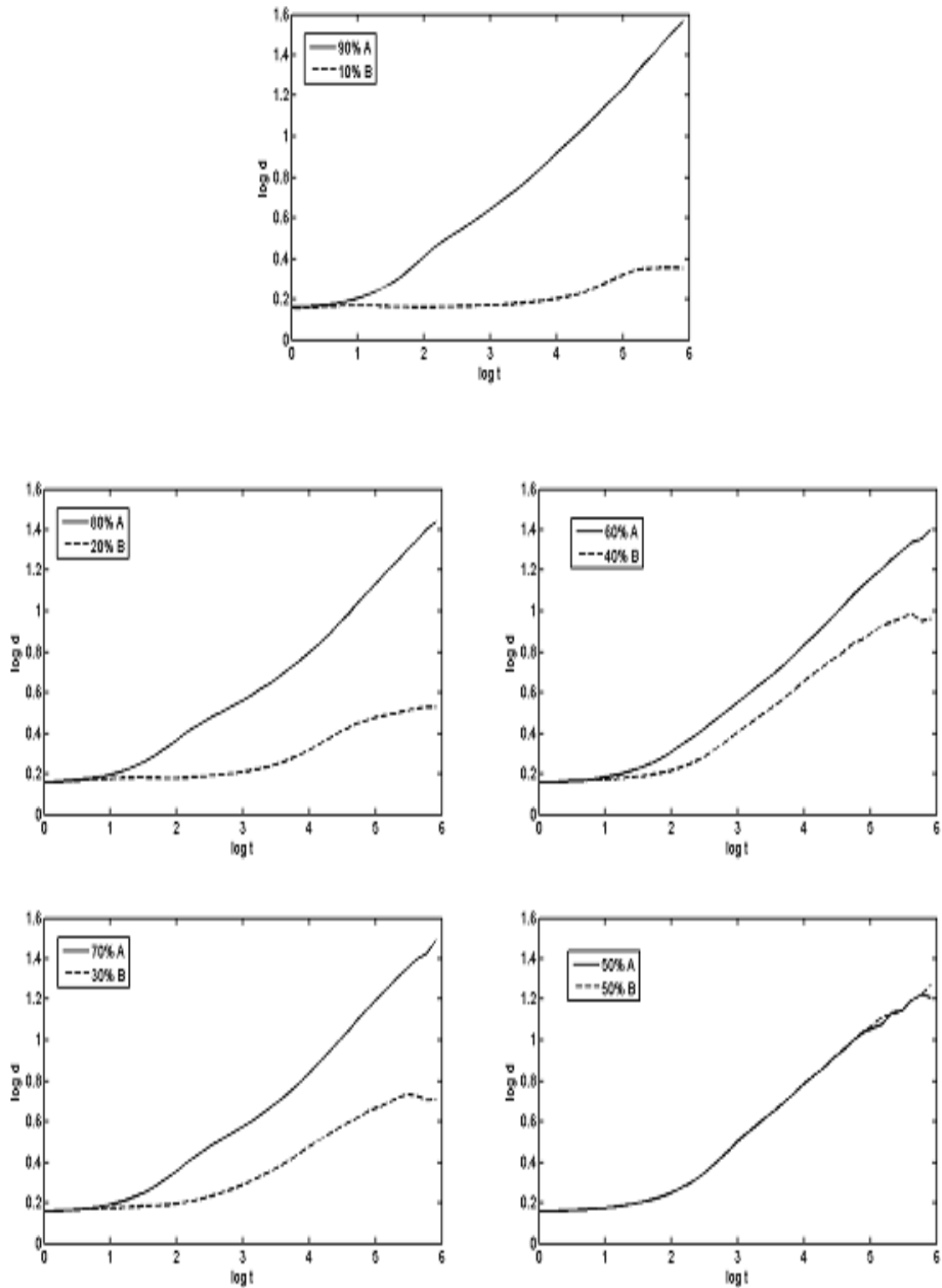


Fig. 3 Dependence of grain size on time. The volume fraction of both phases are indicated.

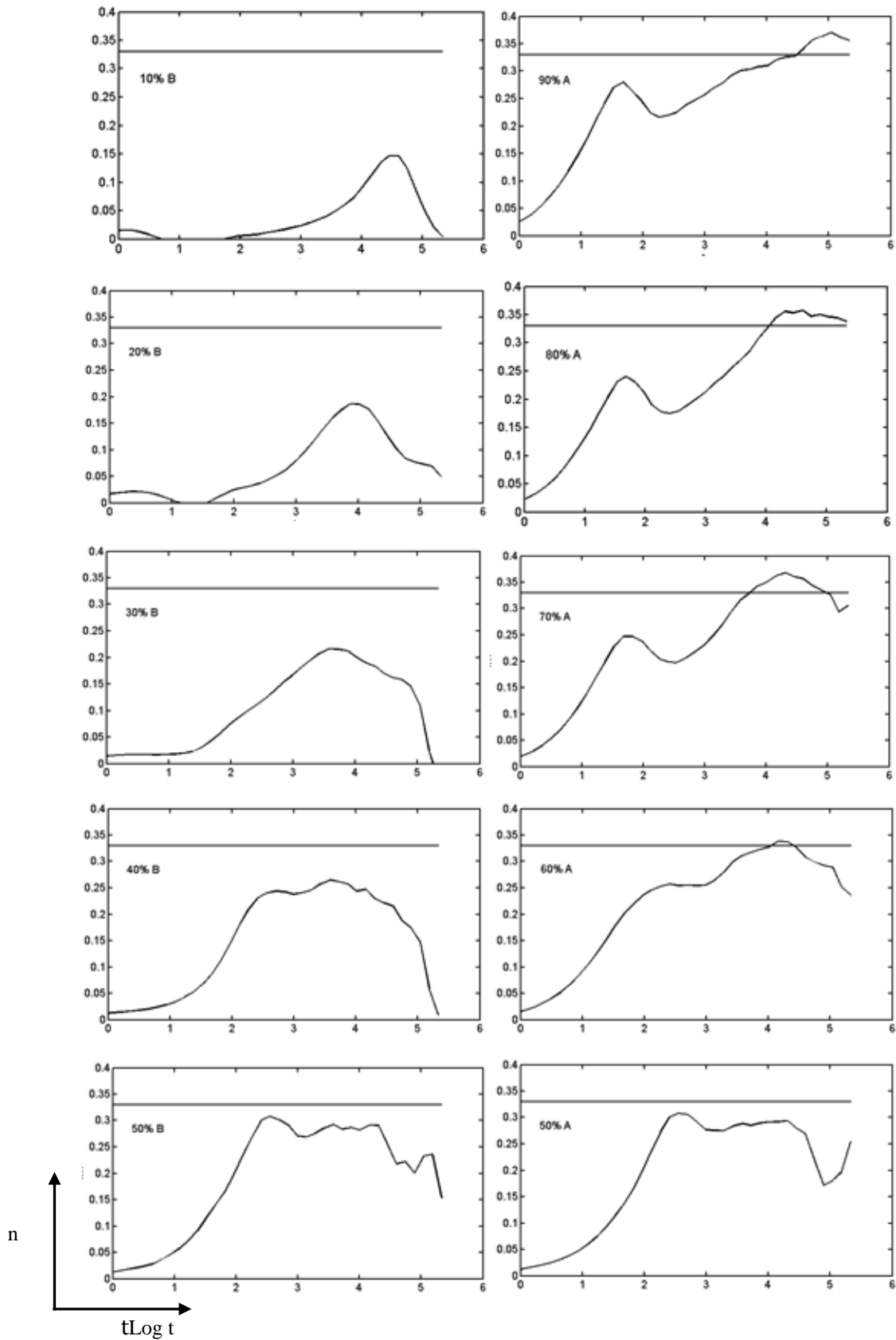


Fig. 4 Dependence of the slope of the curves in Fig. 3 on time for a broad volume fraction range of the B phase. The horizontal solid lines represent the theoretical value $1/n=0.33$ for Ostwald ripening via long-range diffusion.

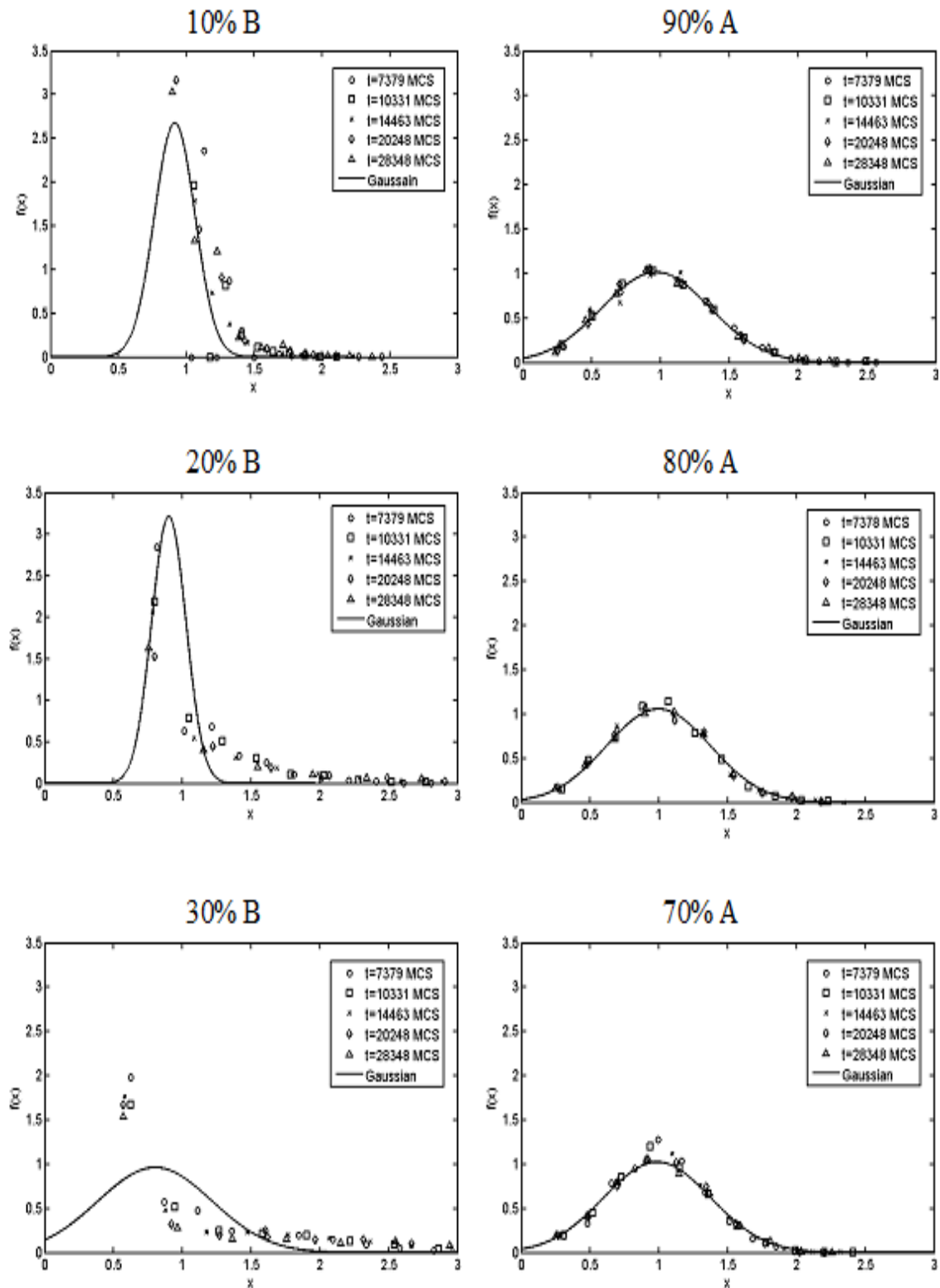


Fig. 5 Effect of volume fraction on the temporal development of the relative grain size distribution of the two phases for five different time steps, comparing with fit of the Gaussian distribution function. The volume fraction of phase B varies between 10%-30% and the volume fraction of phase A varies between 70%-90%.

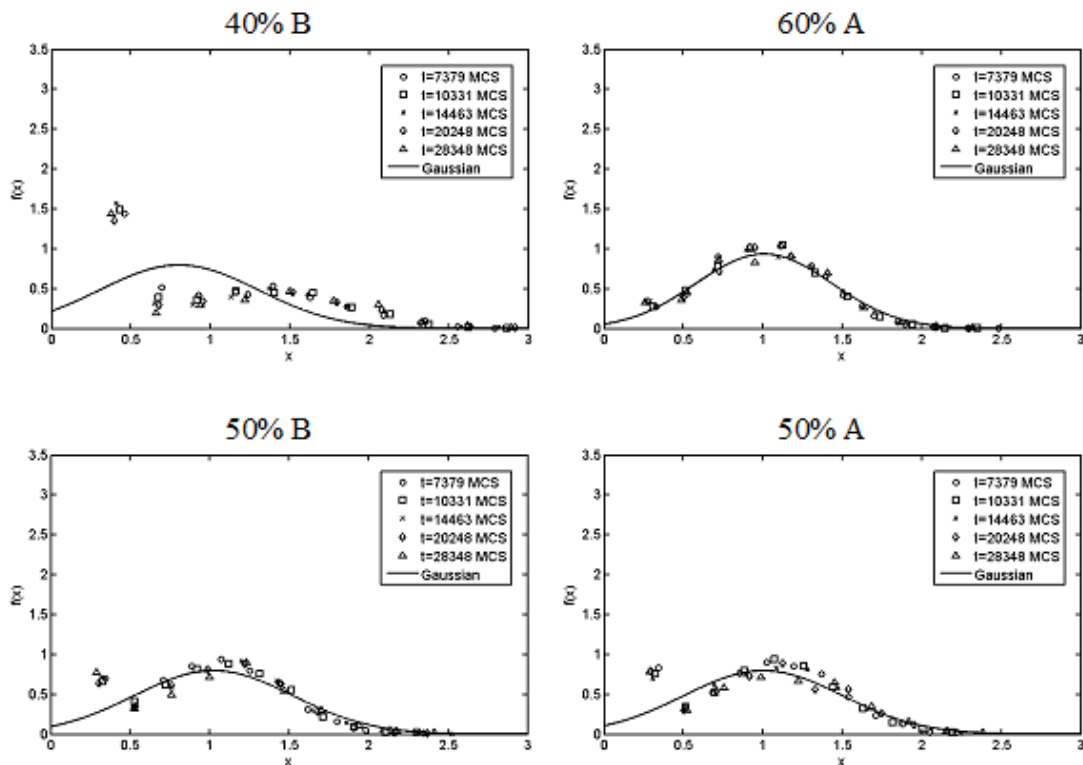


Fig. 6 Effect of volume fraction on the temporal development of the relative grain size distribution of the two phases for five different time steps, comparing with fit of the Gaussian distribution function. The volume fraction of phase B varies between 40%-50% and the volume fraction of phase A varies between 50%-60%.

IV. Conclusion

The Monte Carlo Potts model has been used to simulate the coupling between grain growth and Ostwald ripening in two-phase polycrystalline materials. The suitable value of the ratio between the grain boundary energies to the interphase energies is imbedded as an input parameter in the model. It is found that the microstructural evolution of the two phases reaches a quasi-stationary state at different aging times depending on the volume fractions. The value of the grain growth exponent close to the value of $n=3$ in agreement with the theoretical value of Ostwald ripening for volume fractions between 40% and 90%. Whereas the quasi-stationary state is approached very late near the end of simulation time in the cases of volume fractions between 10% and 30%; therefore, the value of n is larger than 3.

The grain size distribution is analyzed for a broad range of second phase volume fractions. It is found that the grain size distribution vary with the volume fraction. For volume fractions vary between 50% and 90%, the size distributions in the quasi-stationary state are indistinguishable from each other; furthermore, the simulated size distribution within the quasi-stationary state can be described very well by the normal distribution function. The simulated size distributions within the quasi-stationary state are symmetric and peaked at $x=1$. However, for lower volume fractions differ between 10% and 40%, the simulated size distribution within the quasi-stationary state are asymmetric and skew to smaller grains.

References

- [1] P.A. Beck, J.C. Kremer, L.J. Demer, M.L Holzworth, Grain growth in high-purity aluminum and in an aluminum–magnesium alloy, *Trans. AIME*, 175, 1948, 372–394.
- [2] J.E. Burke, Some factors affecting the rate of grain growth in metals, *Trans. Metall. Soc. AIME*, 180, 1949, 73–91.
- [3] J.E. Burke, D. Turnbull, Recrystallization and grain growth, *Prog. Metal. Phys.*, 3, 1952, 220–292.
- [4] I.M. Lifshitz, V.V. Slyozov, The kinetics of precipitation from supersaturated solid solution, *J. Phys. Chem. Solids*, 19, 1961, 35–50.
- [5] C. Wagner, Theorie der alterung von niederschlägen durch umlösen, *Electrochem.*, 65, 1961, 581–591.
- [6] A.J. Ardell, On the coarsening of grain boundary precipitates, *Acta Metall.*, 20, 1972, 601–609.
- [7] M.W. Nordbakke, N. Ryum, and O. Hunderi, Curvilinear polygons, finite circle packings, and normal grain growth, *Materials Science and Engineering A.*, 385, 2004, 229-234.
- [8] D. Zöllner, and P. Streitenberger, Three-dimensional normal grain growth: Monte Carlo Potts model simulation and analytical mean field theory, *Scr. Mater.*, 54, 2006, 1697-1702.
- [9] J.D. French, M.E. Harmer, H.M. Chan, G.A. Miller, Coarsening-resistant dual-phase interpenetrating microstructures, *J. Am. Ceram. Soc.*, 73 (8), 1990, 2508-2510.

- [10] F.F. Lange, and M.M. Hirlinger, Grain growth in two-phase ceramics: Al₂O₃ inclusions in ZrO₂, *J. Am. Ceram. Soc.*, 70(11), 1987, 827-833.
- [11] K. Mader, E. Hornbogen, Systematics of recrystallization micromechanisms in $\alpha + \beta$ brass, *Scripta Metall.*, 8, 1974, 979-984.
- [12] K. Holm, J. D. Embury, G. R. Purdy, The structure and properties of microduplex Zr-Nb alloys, *Acta Metall.*, 25, 1977, 1191-1200.
- [13] G. Grewal, S. Ankem, Particle coarsening behavior of titanium alloys, *Metall. Trans.*, 21A, 1990a, 1645-1654.
- [14] G. Grewal, S. Ankem, Modeling matrix grain growth in the presence of growing second phase particles in two-phase alloys, *Acta Metall.*, 38, 1990b, 1607-1617.
- [15] G.T. Higgins, S. Wiryolukito, P. Nash, The kinetics of coupled phase coarsening in two-phase structures, *Mater. Sci. Forum*, 92-96, 1992, 671-676.
- [16] S. Ankem, Grain growth in multiphase alloys, *Mater. Sci. Forum*, 92-96, 1992, 159-168.
- [17] K.B. Alexander, P.F. Becher, S.B. Waters, A. Bleier, Grain growth kinetics in alumina-zirconia (CeZTA) composites, *J. Am. Ceram. Soc.*, 77, 1994, 939-946.
- [18] D. Fan and L. Q. Chen, Computer simulation of grain growth and Ostwald ripening in Alumina-Zirconia two-phase composites, *J. Am. Ceram. Soc.*, 80, 1997, 1773-1780.
- [19] D. Fan, L.Q. Chen, S.P.P. Chen, Numerical simulation of Zener pinning with growing second-phase particles, *J. Am. Ceram. Soc.*, 81, 1998, 526-532.
- [20] V.S. Solomatov, R. El-Khozondar, V. Tikare, Grain size in the lower mantle: constraints from numerical modeling of grain growth in two-phase systems, *Phys. Earth. Planet. Inter.*, 129, 2002, 265-282.
- [21] El-Khozondar, R., Zöllner, D., Kassner, K.: Numerical simulation of grain size distribution in two-phase polycrystalline materials: International Journal of Materials Science and Applications 3(6), 2014, 381-390.
- [22] R. El-Khozondar, H. El-Khozondar, Monte Carlo Potts simulation of grain growth of solid grains dispersed in a liquid matrix, *Journal of Engineering Research and Technology*, 2(1), 2015, 7-14.
- [23] M.P. Anderson, D.J. Srolovitz, G.S. Grest, P.S. Sahni, Computer simulation of grain growth. I. Kinetics, *Acta Metall.*, 32 (5), 1984, 783-791.
- [24] M.P. Anderson, G.S. Grest, D.J. Srolovitz, Computer simulation of grain growth in three dimensions, *Phil. Mag.*, 59B, 1989, 293-329.
- [25] X. Song, G. Liu, A simple and efficient three-dimensional Monte Carlo simulation of grain growth, *Scr. Mater.*, 38, 1998, 1691-1696.
- [26] V. Tikare, and J.D. Gawlez, Applications of the Potts model to simulation of Ostwald ripening, *J. Am. Ceramic Soc.*, 81, 1998, 485-491.
- [27] P. Blikstein and A. P. Tschiptschin, Monte Carlo simulation of grain growth, *Materials Research*, 2, 1999, 133-137.
- [28] Q. Yu and S.K. Esche, A Monte Carlo algorithm for single phase normal grain growth with improved accuracy and efficiency, *Comput. Mater. Sci.*, 27, 2003a, 259-270.
- [29] Q. Yu and S.K. Esche, Three-dimensional grain growth modeling with a Monte Carlo algorithm, *Mater. Lett.* 57, 2003b, 4622-4626.
- [30] L. Hui, W. Guanghou, D. Feng, B. Xiufang, F. Pederiva, Monte Carlo simulation of three-dimensional polycrystalline material, *Mater. Sci. Eng.*, A 357, 2003, 153-158.
- [31] D. Zöllner and P. Streitenberger, Three-dimensional normal grain growth: Monte Carlo Potts model simulation and analytical mean field theory, *Scr. Mater.*, 54, 2006, 1697-1702.
- [32] D. Zöllner, P. Streitenberger, Monte Carlo Simulation of Normal Grain Growth in Three Dimensions, *Mater. Sci. Forum*, 567, 2008, 81-84.
- [33] D. Zöllner, P. Streitenberger, Grain size distributions in normal grain growth, *Practical Metallography/Praktische Metallographie*, 47, 2010, 618-639.
- [34] R.M German., P. Suri, S.J. Park, Review: liquid phase sintering, *J. Mater. Sci.*, 44, 2009, 1-39.
- [35] R. El-Khozondar, H. El-Khozondar, Numerical simulations of coarsening of lamellar structures: applications to metallic alloys, *Egypt. J. Solids*, 27(2), 2004, 189-199.
- [36] R. El-Khozondar, H. El-Khozondar, G. Gottstein, A. Rollet, Microstructural Simulation of Grain Growth in Two-phase Polycrystalline Materials, *Egypt. J. Solids*, 29(1), 2006, 35-47.
- [37] R. El-Khozondar, H. El-Khozondar, Numerical modeling of microstructural evolution in three-phase polycrystalline materials, *Arab. J. Sci. Eng.*, 34(1A), 2009, 241-252.